Iranian Journal of Chemical Engineering
Vol. 16, No. 4 (2019), IAChE

Modeling of Nanofiltration of Low Concentration Pb(II) Aqueous Solutions Using a Coupled Concentration Polarization and Pore Flow Model

S. Fadhil

Department of Chemical and Petrochemical Engineering, College of Engineering, University of Anbar, Iraq

ARTICLE INFO

Article history:
Received: 2019-05-23
Accepted: 2020-05-28

Keywords:
Membrane,
Nanofiltration,
ENP,
Concentration,
Polarization,
Lead

ABSTRACT

In this paper, the performance of nanofiltration membrane process in removing Pb(II) from aqueous solution was modeled by the pore flow-concentration polarization model. The model was fabricated based on the simultaneous resolving of Extended Nernst–Planck equation(ENP), film theory, and osmotic pressure model. The effects of various operational parameters such as the applied pressure, feed concentration, and cross-velocity on lead Pb(II) ion rejection and solvent flux were investigated. The applied pressure, feed concentration, and cross-velocity varied between 10-50 bar, 5-15 ppm, and 0.2-1.2 m/s, respectively. It was found that lead rejection increased initially and reached the maximum value; then, it decreased with a further increase in pressure, while solvent flux increased linearly within the whole pressure range. This phenomenon is attributed mainly to the developed concentration polarization layer. This effect was significantly decreased with increasing cross-velocity to 1.2 m/s. Ultimately, the proposed model successfully predicted the filtration process in terms of real and observed rejections as well as solvent flux.

1. Introduction

Different technologies have been developed so far to treat water contamination using heavy metals such as ion exchange, Electrodialysis (ED), Nanofiltration (NF), and Reverse Osmosis (RO) [1]. Nanofiltration process is widely used due to its higher performance than other separating methods. High retention index and flux as well as low investment cost were predicted for the commercial and prepared NF membranes [2-8]. As a result, NF is a promising technology for solving major problems relating to metal separation. Recently, many studies that deal with NF-based heavy metal separation have been published [7-13]. Gherasim and Mikulášek studied the influence of operating conditions on the membrane performance to remove polluting and toxic Pb(II) ions from aqueous solutions [9]. They found that the rejection of lead ions was slightly increased by a percentage greater than 98 % with an increase in cross-flow velocity and applied pressure; then, it slightly decreased as feed

*Corresponding author: sufyanfadh@gmail.com

concentration increased. Gherasim et al. reported the performance of commercial NF membranes (AFC 80) in the removal of toxic Pb(II) ions from single and binary aqueous solutions [10]. They found that metal rejections were higher than 98.5 % in optimum operating conditions of trans-membrane pressure in the range of 10–30 bars and feed solutions at pH 5.7 containing 50–80 mg metal/L.

Mikulášek and Cuhorka used similar NF membranes (AFC 40 and AFC 80) for removing toxic Pb(II) ions from aqueous waste water, but at high concentrations [11]. They claimed that the maximum rejection of Pb(II) ions was achieved above 80 % for AFC 40 and 98 % for AFC 80, proving that these NF membranes had real potential for efficient removal of metal ions from highly polluted wastewaters. Similarly, Bouranene studied the performance of another type of nanofiltration membranes (polyamide membrane AFC 30) in removing cobalt and lead ions from aqueous solution [12]. They concluded that the intrinsic rejection rate of cobalt was~97 % and that of lead was ~81 %. Mehdipour et al. investigated the influence of ion interaction on lead removal by a polyamide nanofiltration membrane (NE 4040-90). They found that increasing lead ion concentration resulted in a higher retention of 97.5 % at a constant pressure, while the presence of monovalent cations did not reduce lead ion rejection, significantly [13].

Many studies have been focused on modeling NF membranes using different approaches. Fadhil used extended Nernst-Plank equation to predict the rejection of mono and divalent ions in water desalination [6]. He found that NF membranes separated divalent ions more efficiently than monovalent ions. Banerjee and De studied the nanofiltration of two dye system and salt (NaCl) in a textile effluent using a coupled model of concentration polarization and pore flow model [17]. They emphasized that the removal of dyes through the membrane was significant (more than 90 %), but the salt retention was less than 4 % due to its very high concentration in the textile effluent. Maher et al. optimized operating conditions for maximizing heavy metal rejection of the NF membrane by response surface methodology [19]. According to their results, 93 % of nickel and 86 % of lead ions were eliminated in the optimum condition.

In this study, pore flow-concentration polarization model was used to predict the performance of NF membranes to eliminate lead ions from aqueous solution. The application of these theoretical models in NF is not new [14-19]. However, differences in membrane performance and related important parameters still exist, which need to be elucidated correctly.

2. Mathematical model

Donnan Steric Pore-flow (DSPM) model was applied to describing Pb(II) transfer through membrane pores, whereas solute transfer through concentration boundary layer was modeled using film theory [20].

2.1. Solute transfer through concentration polarization layer

Permeate flux through Concentration Polarization (CP) layer can be expressed as [16]:

$$v_w = k \ln\left[\frac{c^m - C_p}{C_o - C_p}\right] \quad (1)$$

where c^m is the concentration in the membrane (mol/m³), and C_p and C_o are concentrations of ion in permeate and at membrane entrance, respectively.

The mass transfer coefficient (k) for turbulent flow can be determined using the following empirical correlation [10]:

$$Sh = 0.023\ Re^{0.875} Sc^{0.25}$$

where Sh, Re, and Sc are Sherwood number, Reynould number, and Schmidt number, respectively.

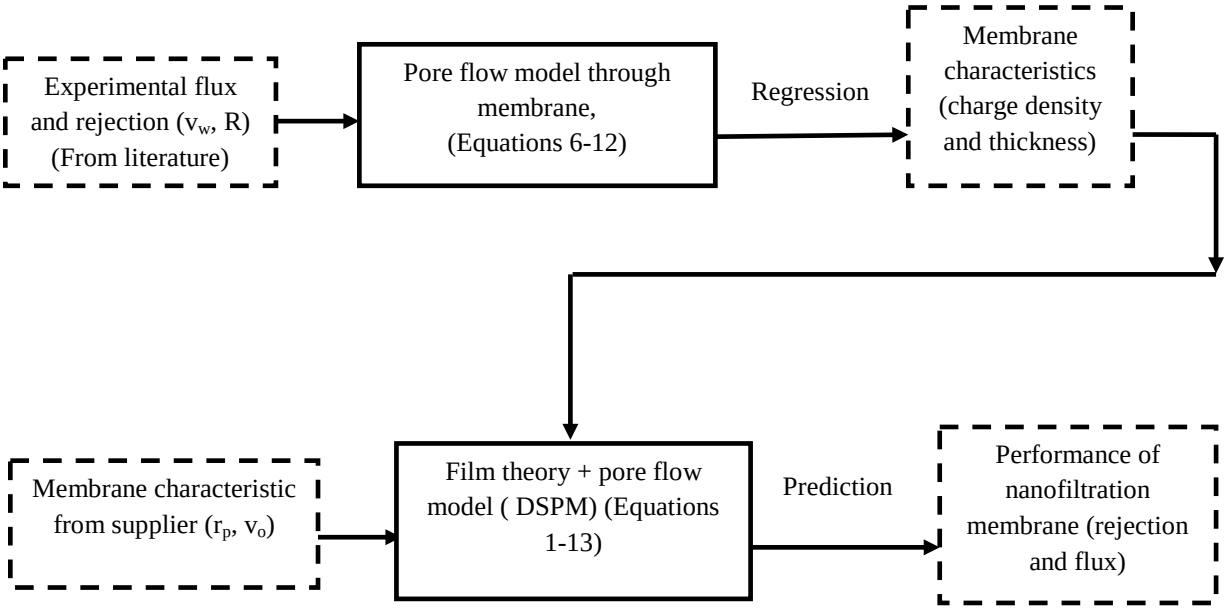

Figure 1. Schematic diagram of the calculations conducted through this study.

2.2. Solvent transfer through membrane layer

By using a modified osmotic pressure model, permeate flux (v_w) can be determined [20]:

$$v_w = \frac{\Delta P - \Delta\pi}{\mu[R_m + R_{ads}]} \quad (2)$$

With low feed concentration, resistance due to adsorption layer (R_{ads}) is assumed to be negligible.

Osmotic pressure $\Delta\pi$ can be calculated by:

$$\Delta\pi = \pi_m - \pi_p \quad (3)$$

Moreover, π_m can be determined by using linear Vant Hoff's relationship:

$$\pi = aC \quad (4)$$

where C is solute concentration on the membrane surface and permeate side and a is the osmotic coefficient:

$$a = \frac{RT}{M} \quad (5)$$

where R is the gas constant (J/mol.K), T is the absolute temperature (K), and M is the molecular weight.

2.3. Solute transfer through the membrane

Pb(II) ion transport through membrane pore can be predicted using Donnan Steric Pore-flow (DSPM) model based on ENP equation:

$$\frac{dc_i^m}{dx} = \frac{v_w}{K_{i,d} D_{i,\infty}} \left(K_{i,c} c_i^m - c_{i,p}\right) - z_i c_i^m \frac{F}{RT} \frac{d\psi^m}{dx} \quad (6)$$

where $D_{i,\infty}$ is the hindered diffusivity (m^2/s), c^m_i is the concentration in the membrane (mol/m^3), z_i is the valence of ion (i), $K_{i,c}$ and K_{id} are the hindrance factor for convection and diffusion, respectively, inside the membrane, R is the gas constant (J/mol.K), T is the absolute temperature (K), F is Faraday constant (C/mol), and ψ is the electrical potential (V) [21].

$K_{i,c}$ and K_{id} are calculated using the following equations [22]:

$$K_{d_i} = 1.0 - 2.30\,\lambda_i + 1.154\lambda_i^2 + 0.224\lambda_i^3$$

$$K_{c_i} = 1.0 + 0.054\,\lambda_i - 0.988\lambda_i^2 + 0.441\lambda_i^3$$

$$\lambda_i = \frac{r_i}{r_p}$$

To get the potential gradient (ψ), the following assumption was applied:

1. The electro-neutrality conditions on feed and permeate sides:

$$\sum_i z_i c_i = 0 \quad (7)$$

2. The electro-neutrality conditions in the membrane:

$$\sum_i (z_i c_i^m) + z_x c_x^m = 0 \quad (8)$$

where z_x, c_x^m are the membrane valance and membrane charge density, respectively.

3. No electric current is flowing across the membrane:

$$\sum_i F z_i J_i = 0 \quad (9)$$

Applying Equations (7-9) to Equation (6) gives the electrical potential gradient as follows:

$$\frac{d\psi^m}{dx} = \frac{\sum_{i=1}^{2} \frac{z_i v_w}{K_{i,d} D_{i,\infty}} (K_{i,c} c_i^m - c_{i,p})}{\frac{F}{RT} \sum_{i=1}^{2} (z_i^2 c_i^m)} \quad (10)$$

The distribution of co-ions (C_B) between the solution and the membrane is expressed in terms of the effective membrane charge density (c_x^m) [23]:

$$\frac{c_B^m}{c_B} = \left(\frac{|z_B| c_B}{|z_B| c_B^m + |z_x| c_x^m|} \right)^{|z_B|/|z_A|} \quad (11)$$

The observed retention (R_O) of ion (i) is given as:

$$R_O = 1 - \frac{c_{i,p}}{c_{i,f}} \quad (12)$$

where $C_{i,p}$ and $C_{i,f}$ are concentrations of ion on permeate and feed sides, respectively, whereas, the true retention (R_T) of ion is given as follows:

$$R_T = 1 - \frac{c_{i,p}}{C_m} \quad (13)$$

3. Simulation

MATLAB function *FSOLVE* was used to solve the non-linear equation of concentration polarization layer, while fourth-order Rang-Kutta method was used to solve non-linear differential equations to get ions concentrations though membranes. Iterative procedure was conducted to solve these equations to obtain ion concentration on the permeate side with tolerance of 10^{-5}. The input parameters for the model are listed in Table 1. The accuracy of the model predictions was determined by calculating χ^2 parameter using the following formula [24]:

$$\chi^2 = \sum \frac{(R_{exp} - R_{cal})^2}{R_{cal}}$$

where R_{exp} and R_{cal} are lead experimental and calculated rejections, respectively. Small χ^2 value (<1) indicates that experimental results are well fitted by the proposed model.

4. Results and discussion

The simulated rejection of Pb(II) reveals a steady behavior with good agreement with the experimental data reported by Gherasim and Mikulášek using tubular NF membrane (AFC 80) (Fig. 2) [9]. The small value of χ^2 (0.899) implies high accuracy of the numerical calculations and proves the feasibility of the modeling approach. The slight discrepancy between the modeling predictions and the experimental data may be attributed to the fact that solution is considered pure solvent with viscosity of pure solvent. This is a simplification, because in reality there is a difference in concentration along the boundary layer and as a consequence a viscosity difference as well [25]. Moreover, an assumption of negligible lead adsorption used to solve the osmotic pressure equation may not be reliable even at low Pb(II) concentrations.

Table 1
Main characteristics of AFC 80 (PCI Membrane Systems) and operating conditions.

Membrane structural parameter		Data origin
Membrane type	Thin film composite, tubular	supplier
Material	Aromatic polyamide skin layer on polysulfone substrate	supplier
Operating pressure (bar)	0-60	supplier
Operating temperature (°C)	0-70	supplier
Feed pH range	1.5-10.5	Supplier
Membrane surface charge	Negative	supplier
Membrane charge density (mol/m^3)	280	Regression of experimental data
NaCl rejection (%)	80	supplier
Mean pore radius (nm)	0.262	[10]
Thickness to porosity ratio	6.32	[10]
Water permeability (v_o) (L/m^2h)	1.45	[10]
Isoelectric point	3.6	[10]

The effect of feed concentration and cross velocity on observed rejection is shown in Fig. 3. It is clear that lead retention increases significantly with feed velocity until reaching a steady state value for each feed concentration. Different hypotheses were suggested to elucidate this behavior [9, 15, 26]. However, It seems that a combination effect of increasing mass transfer coefficient at the polarization layer (k) as cross-flow velocity increases. In addition, retention generally decreases with feed concentration. At lower lead concentrations (<100 ppm), lead retention by the charge exclusion mechanism is insignificant since lead adsorption is negligible at high feed velocity. Moreover, the steric exclusion mechanism seems to be more important than charge effect because lead ion size is approximately equal to pore radius. Therefore, the effect of feed concentration on the decline of Pb(II) retention is attributed to increasing osmotic pressure, resulting in permeate flux decline and the retention is also decreasing because less solvent is passing through the membrane.

Figure 4 shows the real retention of Pb(II) at different feed concentrations and velocities. The maximum retention percentages of Pb(II) are 97.59 %, 96.7 %, and 95.6 % at feed concentrations of 5, 10, and 15 ppm, respectively. This is in agreement with experimental results reported in the literature, where solute rejection decreases with concentration [9,15,27].

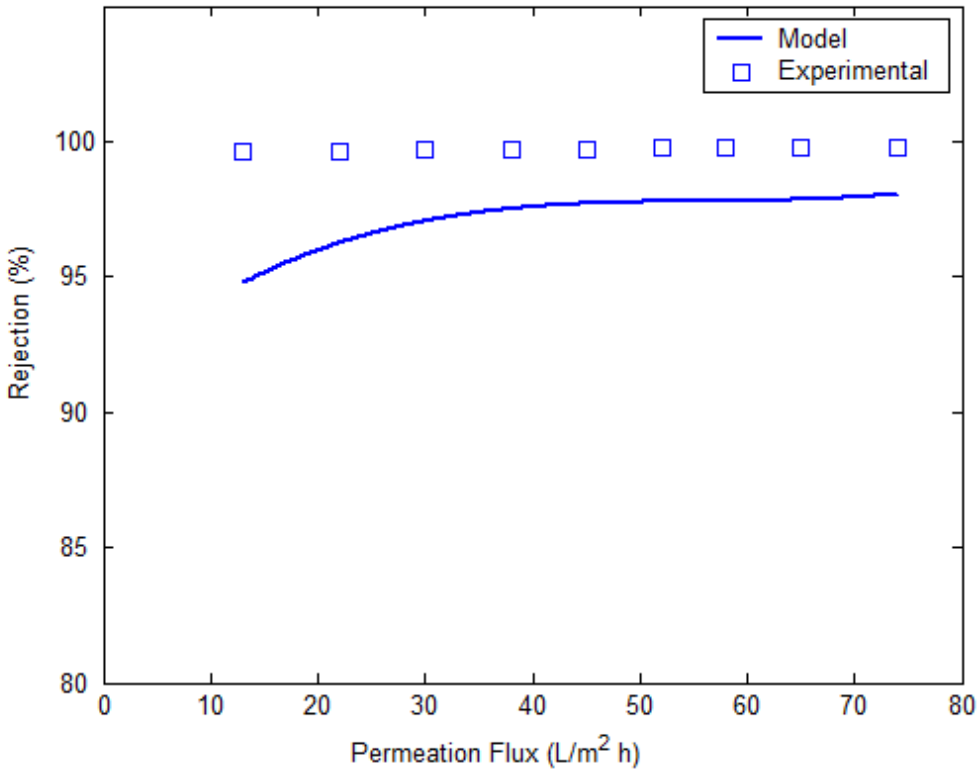

Figure 2. Comparison of rejection of Pb obtained from experiments and performance prediction simulations for AFC 80 NF membranes at feed concentration of 5 ppm and feed velocity of 1.2 m/s.

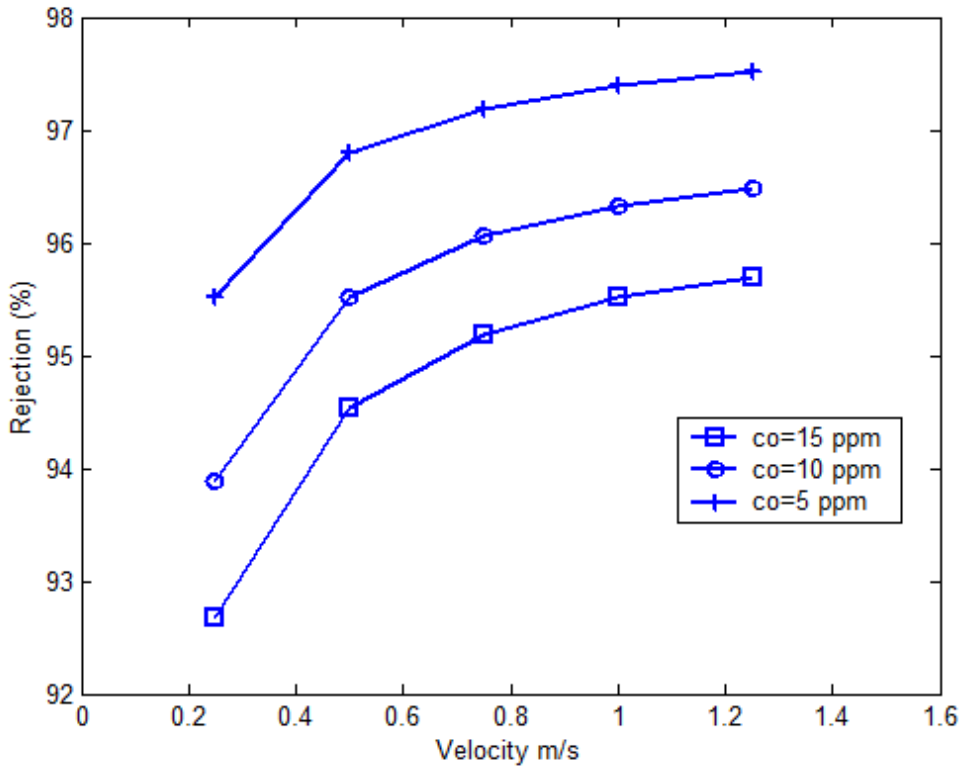

Figure 3. Observed rejection of Pb obtained from performance prediction simulations for AFC 80 NF membrane at pressure 50 bar and different feed concentrations.

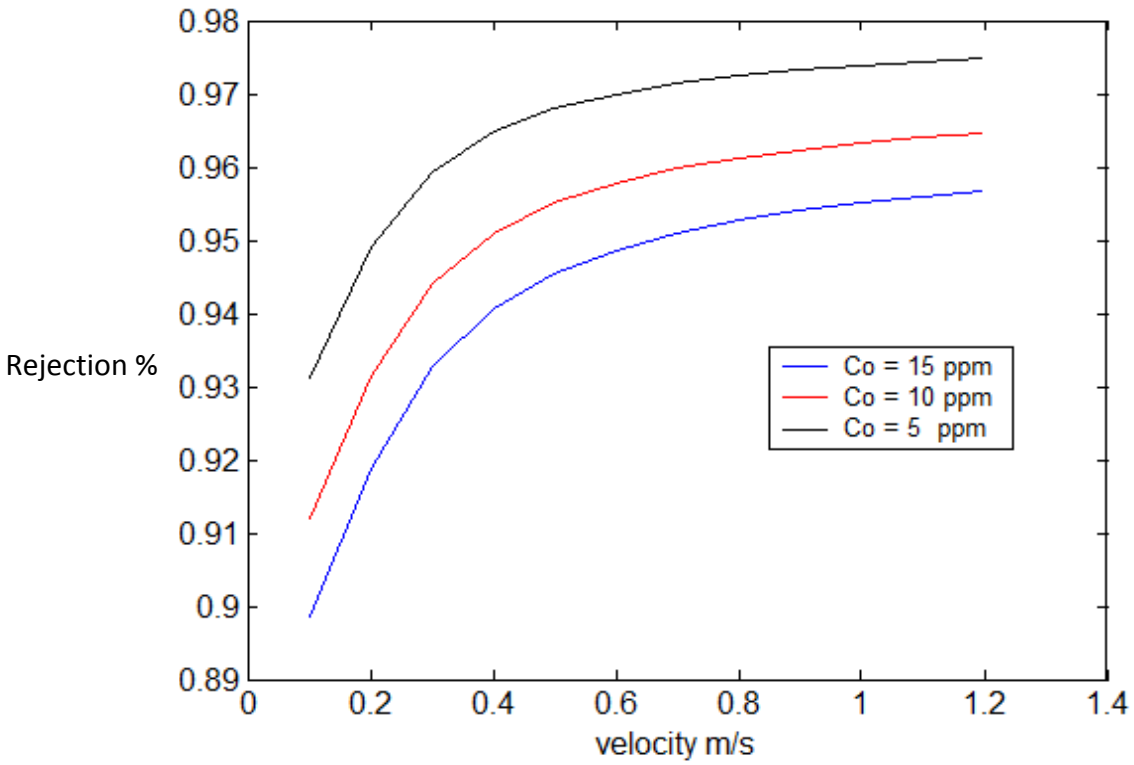

Figure 4. Real rejection of Pb obtained for AFC 80 NF membrane at pressure 50 bar and different feed concentrations and velocities.

Due to the effect of concentration polarization layer, higher real retention values have been obtained than actual retention values (Figure 3). Furthermore, at higher pressure (50 bar), the concentration polarization is significant and a more selective layer onto the membrane surface is formed [14]. On the other hand, by increasing feed pressure, the overall mass transfer coefficient decreases due to high CP resistance [28]. However, the difference between the concentration of Pb in the bulk and that on the membrane surface decreases significantly at a velocity higher than 0.6 m/s at different feed concentrations (Figure 5). These suggested that the concentration polarization influence decreased at high feed velocities [20].

The predicted permeate flux and observed rejection of Pb(II) versus applied pressure are shown in Fig. 6. For $Pb(NO_3)_2$ solution with a concentration of 15 ppm, permeate flux increases linearly with pressure even at high pressure where concentration polarization effect is significant (Fig. 7). On the other hand, the observed rejection of Pb(II) changes with applied pressure. The rejection of Pb(II) increases initially and reaches the maximum of 94 % at pressure of 30 bar and then, declines with further increased pressure; due to concentration polarization effect, a similar result was observed for ion separation by NF membranes [13,15,20,29].

When the applied pressure increased, two phenomena would occur at the same time; more solute is forced to the membrane surface that results in concentration polarization and solute rejection will be decreased. Second, the solvent flux will be increased; however, the solute transport across the membrane is hindered by steric and electrical effects [10,20].

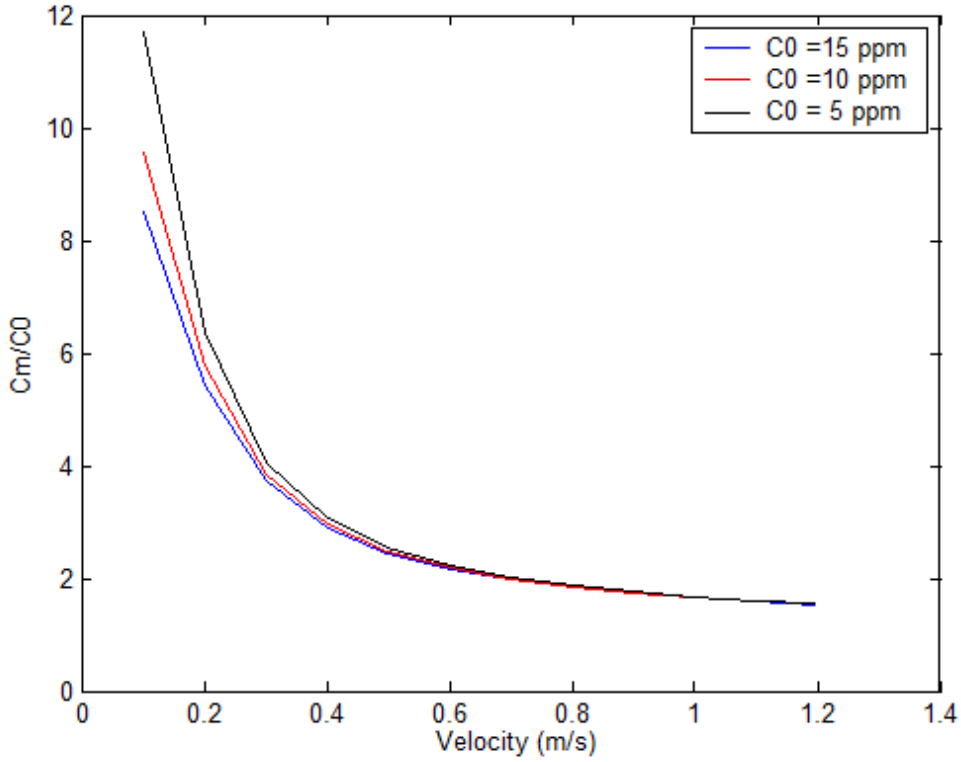

Figure 5. Ratio of Pb concentration on the membrane surface to Pb concentration on the bulk side for AFC 80 NF membrane at pressure 50 bar and different feed concentrations and velocities.

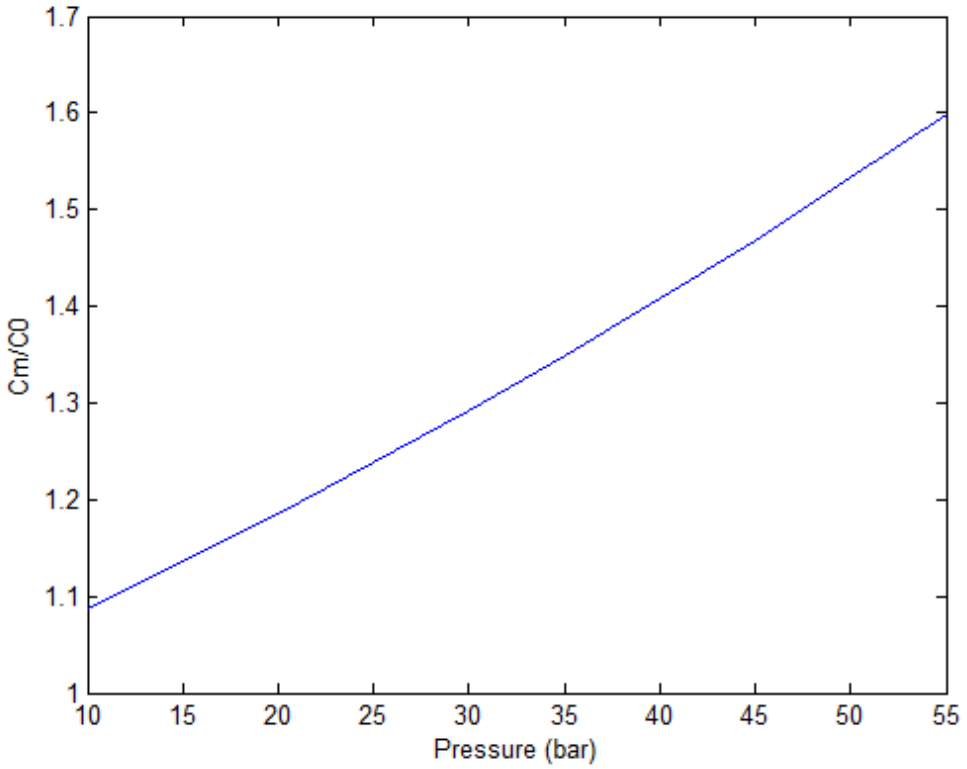

Figure 6. Ratio of Pb concentration on membrane surface to Pb concentration on bulk side vs. pressure for AFC 80 NF membrane at 5 ppm and 1.25 m/s.

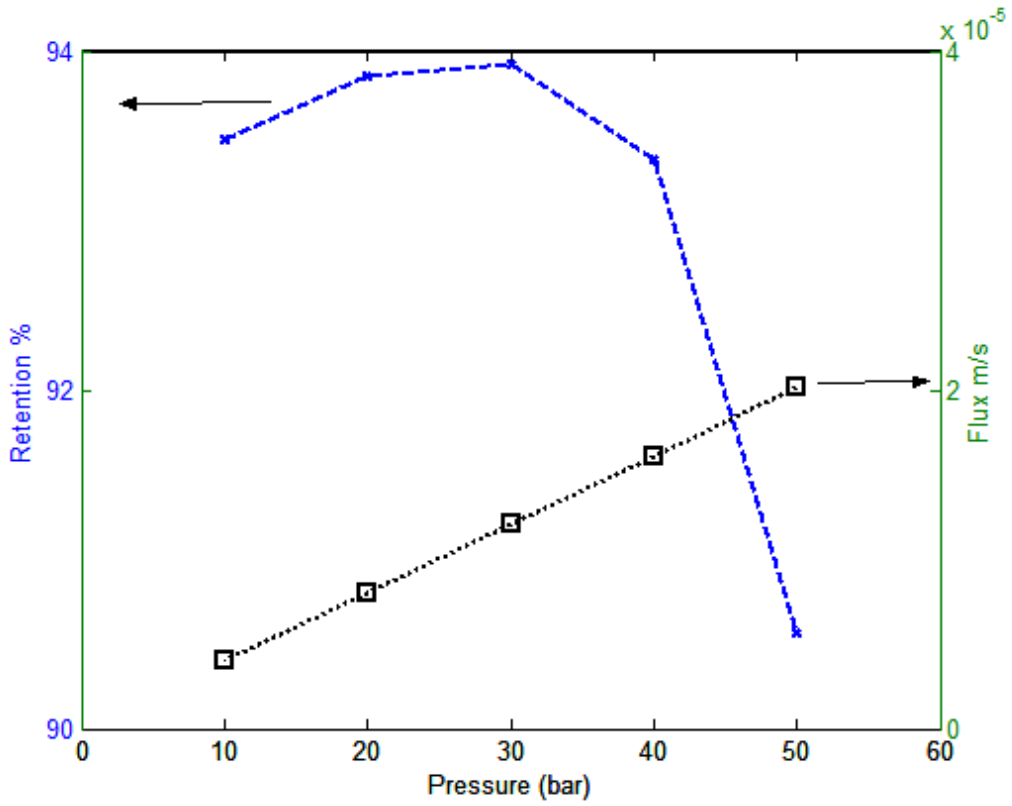

Figure 7. Observed retention of Pb and permeate flux obtained for AFC 80 NF membrane at 5 ppm and 1.2 m/s.

5. Conclusions

In this study, a prediction based on modified ENP equation was presented to quantify the observed and real rejection of Pb(II) ions, as well as permeate flux in the presence of concentration polarization effect. The calculated observed rejection was in good agreement with experimental data. It was found that the lead ion rejection was dependent mainly on feed concentration, the applied pressure, and feed velocity. At the pressure of 30 bar with lead concentration of 5 ppm, the maximum observed retention was 94 %. As feed velocity increased, observed and real rejections increased due to decrease in concentration polarization on the membrane surface. It was also observed that with increase in feed concentration, the observed and real rejections decreased significantly due to the high degree of concentration polarization. Finally, at a feed concentration of 5 ppm and a feed velocity of 1.2 m/s, the observed rejection declined as pressure exceeded 30 bar due to simultaneous effects of concentration polarization and high solvent flux.

References

[1] Gunatilake, S. K., "Methods of removing heavy metals from industrial wastewater", *Journal of Multidisciplinary Engineering Science Studies (JMESS)*, **1** (1), 12 (2015).

[2] van der Meer, W. G. J., Averink, C. W. A. and van Dijk, J. C., "Mathematical model of nanofiltration systems", *Desalination*, **105**, 25 (1996).

[3] Wiesner, M. R. and Chellam, S., "The promise of membrane technology", *Environ. Sci. Technol.*, **33** (17), 360A

(1999).

[4] Bian, R., Yamamoto, K. and Watanabe, Y., "The effect of shear rate on controlling the concentration polarization and membrane fouling", *Desalination*, **131**, 225 (2000).

[5] Sablani, S. S., Goosen, M. F. A., Al-Belushi, R. and Wilf, M., "Concentration polarization in ultrafiltration and reverse osmosis: A critical review", *Desalination*, **141**, 269 (2001).

[6] Fadhil, S., "Performance of nanofiltration membranes on water demineralization assessment and comparative study", *Indian Journal of Chemical Technology*, **6** (4),178 (2018).

[7] Algebory, S., Figoli, A., Alsalhy, Q., Alwan, G. and Simone, S., "Polyvinyl alcohol/Polyvinyl chloride (Pva/Pvc) hollow fiber composite nanofiltration membranes for water treatment", *Iraqi Journal of Chemical and Petroleum Engineering*, **11** (4), 23 (2010).

[8] Alsalhy, Q., Algebory, S., Alwan, G., Simone, S. and Figoli, A., "Hollow fiber ultrafiltration membranes from poly (vinyl chloride): Preparation, morphologies, and properties", *Separation Science and Technology*, **46** (14), 2199 (2011).

[9] Gherasim, C. and Mikulášek, P., "Influence of operating variables on the removal of heavy metal ions from aqueous solutions by nanofiltration", *Desalination*, **343**, 67 (2014).

[10] Gherasim, C., Cuhorka, J. and Mikulasek, P., "Analysis of lead(II) retention from single salt and binary aqueous solutions by a polyamide nanofiltration membrane: Experimental results and modeling", *Journal of Membrane Science*, **436**, 132 (2013).

[11] Mikulášek. P. and Cuhorka, J., "Removal of heavy metal ions from aqueous solutions by nanofiltration", *Chemical Engineering Transaction*, **47**, 379 (2016).

[12] Bouranene, S., Fievet, P., Szymczyk, A., Samar, M. and Vidonne, A., "Influence of operating conditions on the rejection of cobalt and lead ions in aqueous solutions by a nanofiltration polyamide membrane", *Journal of Membrane Science*, **325**, 150 (2008).

[13] Mehdipour, S., Vatanpour, V. and Kariminia, H., "Influence of ion interaction on lead removal by a polyamide nanofiltration membrane", *Desalination*, **362**, 84 (2015).

[14] Giacobbo, A., Bernardes, A., Rosa, M. and de Pinho, M., "Concentration polarization in ultrafiltration/ nanofiltration for the recovery of polyphenols from winery wastewaters", *Membranes*, **8**, 46 (2018).

[15] Otero-Fernández, A., Otero, J., Maroto-Valiente, A., Calvo, J., Palacio, L., Prádanos, P. and Hernández, A., "Reduction of Pb(II) in water to safe levels by a small tubular membrane nanofltration plant", *Clean Techn. Environ. Policy*, **20**, 329 (2018).

[16] Banerjee, P. and De, S., "Steady state modeling of concentration polarization including adsorption during nanofiltration of dye solution", *Separation and Purification Technology*, **71**, 128 (2010).

[17] Banerjee, P. and De, S., "Coupled concentration polarization and pore flow modeling of nanofiltration of an industrial textile effluent", *Separation and Purification Technology*, **73**, 355 (2010).

[18] Yang, G., Xing, W. and Xu, N., "Concentration polarization in spiral-wound nanofiltration membrane elements", *Desalination*, **154**, 89 (2003).

[19] Maher, A., Sadeghi, M. and Moheb, A., "Heavy metal elimination from drinking water using nanofiltration membrane technology and process optimization using response surface methodology", *Desalination*, **352**, 166 (2014).

[20] Banerjee, P. and De, S., "Modeling of nanofiltration of dye using a coupled concentration polarization and pore flow model", *Separation Science and Technology*, **46**, 561 (2011).

[21] Gozálvez-Zafrilla, J. and Santafé-Moros, A., "Nanofiltration modeling based on the extended Nernst-Planck equation under different physical modes", Proceedings of *The COMSOL Conference*, Hannover, Germany, (2008).

[22] Perez Gonzalez, A., Ibáñez, R., Gómez, P., Urtiaga, A., Ortiz, I. and Irabien, J., "Nanofiltration separation of polyvalent and monovalent anions in desalination brines", *J. of Memeb. Sci.*, **473**, 16 (2015).

[23] Lakshminarayanaiah, N., Transport Phenomena in Membranes, Academic Press, New York, (1969).

[24] Foo, K. and Hameed, B., "Insights into the modeling of adsorption isotherm systems", *Chem. Eng. J.*, **156**, 2 (2010).

[25] Peshev, D. and Livingston, A., "OSN designer, a tool for predicting organic solvent nanofiltration technology performance using Aspen One, MATLAB and CAPE OPEN", *Chemical Engineering Science*, **104**, 975 (2013).

[26] Rios, G. and Joulie, R., "Investigation of ion separa-tion by microporous nanofiltration membranes", *AIChE J.*, **42** (9), 2521 (1996).

[27] De´on, S., Dutournie´, P. and Bourseau, P., "Modeling nanofiltration with Nernst-Planck approach and polarization layer", *AIChE J.*, **53** (8), 1952 (2007).

[28] Rafia, N., Beiragh, M. and Babaluo, A., Current trends and future developments on (bio-) membranes, Elsevier, Holland, Chap. 14, (2017).

[29] Rall, D., Menne, D., Schweidtmann, A., Kamp, J., Kolzenberg, L., Mitsos, A. and Wessling, M., "Rational design of ion separation membranes", *Journal of Membrane Science*, **569**, 209 (2019).